Article

Joint Analysis of Cardiovascular Control and Shear Wave Elastography to Determine Carotid Plaque Vulnerability [†]

Vlasta Bari [1,2,*], Beatrice Cairo [1], Francesca Gelpi [2], Fabiana Fancoli [3], Nicoletta Curcio [4], Giulia Matrone [5], Paolo Righini [3], Giovanni Nano [1,3], Alberto Porta [1,2] and Daniela Mazzaccaro [3]

1   Department of Biomedical Sciences for Health, University of Milan, 20133 Milan, Italy;
    beatrice.cairo@unimi.it (B.C.); giovanni.nano@unimi.it (G.N.); alberto.porta@unimi.it (A.P.)
2   Department of Cardiothoracic, Vascular Anaesthesia and Intensive Care, IRCCS Policlinico San Donato,
    20097 San Donato Milanese, Italy; francesca.gelpi@grupposandonato.it
3   Operative Unit of Vascular Surgery, IRCCS Policlinico San Donato, 20097 San Donato Milanese, Italy;
    fabiana.fancoli@grupposandondato.it (F.F.); paolo.righini@grupposandonato.it (P.R.);
    daniela.mazzaccaro@grupposandonato.it (D.M.)
4   3D and Computer Simulation Laboratory, IRCCS Policlinico San Donato, 20097 San Donato Milanese, Italy;
    nicoletta.curcio@grupposandonato.it
5   Department of Electrical, Computer and Biomedical Engineering, University of Pavia, 27100 Pavia, Italy;
    giulia.matrone@unipv.it
*   Correspondence: vlasta.bari@unimi.it; Tel.: +39-02-52774381
†   This article is a revised and expanded version of a paper entitled "Joint analysis of baroreflex control and
    shear wave elastography to assess the vulnerability of carotid artery plaque". Reference: Bari, V.; Gelpi, F.;
    Cairo, B.; Fancoli, F.; Curcio, N.; Matrone, G.; Nano, G.; Porta A.; and Mazzaccaro, D. Joint analysis of
    baroreflex control and shear wave elastography to assess the vulnerability of carotid artery plaque, in
    Computing in Cardiology. **2024**, *10*, 1–4.

Abstract: Background/Objectives: Carotid artery stenosis (CAS) is one of the main causes of stroke, and the vulnerability of plaque has been proved to be a determinant. A joint analysis of shear wave elastography, a radiofrequency echo-based wall tracking technique for arterial stiffness evaluation, and of autonomic and baroreflex function is proposed to noninvasively, preoperatively assess plaque vulnerability in asymptomatic CAS patients scheduled for carotid endarterectomy. **Methods**: Elastographic markers of arterial stiffness were derived preoperatively in 78 CAS patients (age: 74.2 + 7.7 years, 27 females). Autonomic and baroreflex markers were also assessed by means of an analysis of the beat-to-beat fluctuations in heart period and systolic arterial pressure, derived at rest in supine position (REST) and during active standing. Postoperative analysis identified 36 patients with vulnerable plaque (VULN) and 42 with stable plaque (STABLE). **Results**: Baroreflex sensitivity (BRS) at a respiratory rate decreased during STAND only in VULN patients, being much higher at REST compared to STABLE levels. Autonomic indexes were not helpful in separating experimental conditions and/or populations. The Young's modulus (YM) of the plaque was lower in the VULN group than in the STABLE one. Cardiovascular control and elastographic markers were significantly correlated only in VULN patients. A multivariate logistic regression model built combining YM and BRS at the respiratory rate improved the prediction of plaque vulnerability, reporting an area under the ROC curve of 0.694. **Conclusions**: Noninvasive techniques assessing shear wave elastography and baroreflex control could contribute to the early detection of plaque vulnerability in patients with asymptomatic CAS.

Keywords: baroreflex; autonomic nervous system; elastography; Young's modulus; carotid artery stenosis; carotid plaque vulnerability

1. Introduction

Carotid artery stenosis (CAS) as a consequence of atherosclerotic plaque presence is one of the main causes leading to stroke [1,2]. Symptomatic CAS is usually treated with carotid endarterectomy (CEA) or stenting and with medical therapies. The management of asymptomatic CAS is instead more uncertain, since trials reporting the effectiveness of surgery in these patients date back 20 years ago or more, while recent improvements suggest that medical therapy could be as beneficial as CEA or stenting to prevent stroke [3,4]. In particular, the presence of neurologic symptoms such as stroke or transient ischemic attack in a patient with symptomatic carotid stenosis contributes to the vulnerability of the patient, since it has been extensively reported in the literature that symptomatic patients have a higher risk of stroke recurrence. In such patients, the indication of carotid revascularization is straightforward to prevent any further possible neurologic complication. In asymptomatic patients, however, assuming the same degree of stenosis for all patients (i.e., >70%), vulnerability can be defined only via the histologic analysis of the plaque [5].

As a matter of fact, it has been shown that the risk of stroke in asymptomatic CAS is more related to the structure of the atherosclerotic plaque, with some plaques being more vulnerable and prone to rupture than more stable ones [6]. The vulnerability of the plaque would thus be directly linked to the occurrence of stroke [7], but the gold standard technique used to assess plaque vulnerability has so far been considered postoperative histological analysis [8]. As a consequence, identifying vulnerable plaque at an early stage has become more and more important, especially by means of noninvasive techniques [5,9].

Markers of arterial stiffness as assessed via pulse wave velocity have been found to be useful to assess atherosclerosis [10], while other works have identified the ability of imaging, such as computed tomography angiography, magnetic resonance scans, or 2D duplex ultrasound, to identify the characteristics of atherosclerotic plaques [11,12]. However, there is a need for more advanced technologies to also assess the characteristics of plaque vulnerability.

In this direction, ultrasound elastography and, in particular, strain and shear wave elastography, have been suggested as able to identify the mechanical properties of the vascular system, more specifically the elastic properties of the carotid walls, according to the paradigm that higher-stiffness regions are linked to the presence of calcifications, while lower-stiffness regions are linked to soft or hemorrhagic tissue and hence to a more vulnerable plaque [13,14]. In this sense, shear wave elastography (SWE) has been proposed as a noninvasive imaging technique able to identify carotid plaque elasticity [15] and vulnerability, as compared to traditional histology [16]. A preliminary study by our group has also shown that point SWE (pSWE) allowed for the discrimination of patients with vulnerable plaque [17].

Autonomic nervous system function and cardiovascular control, which can be non-invasively assessed from the study of spontaneous fluctuation in heart period (HP) and systolic arterial pressure (SAP), have been found to be depressed in cases of increased cardiovascular risk [18,19]. Several studies have linked the state of autonomic nervous system control to the incidence of cerebrovascular adverse events, like microinfarct or stroke, after a surgical procedure; either vascular or cardiac surgery and their likelihood is also dependent on the age of the patients. As an example, a greater blood pressure variability, usually associated with a dysfunction in baroreflex control, has been associated with a more rapid cognitive decline and a higher likelihood of silent stroke, especially in the elderly [20,21]. Furthermore, reduced autonomic control has been linked to stroke severity [22,23] and to an increased risk of mortality after cerebral ischemia [24].

Such markers have also been proposed to characterize the state of patients with CAS and the surgical impact of CEA [25,26], finding that cardiovascular control was

compromised in patients undergoing CEA [26]. As to the relationship of autonomic function with carotid plaque, it has been reported that the presence of carotid atherosclerotic plaque was associated with a reduced heart rate variability [27], but how cardiovascular control can be linked to plaque vulnerability has not been investigated so far.

We hypothesize that the investigation of autonomic control and especially cardiac baroreflex, the mechanism adjusting variations in HP in response to variations in SAP [28,29], could help in differentiating patients with vulnerable plaque and that the addition of such analysis to ultrasound pSWE, which has already been proved useful in identifying patients with vulnerable plaque, and to arterial stiffness evaluation could further improve risk stratification.

Hence, the aim of this research was to study cardiovascular control by means of a joint analysis of variability series of HP and SAP during a postural challenge and by the elastographic characteristics of the carotid plaque, as derived from pSWE and from ultrasound radiofrequency (RF) echo-based wall tracking in the same cohort of patients with asymptomatic CAS scheduled for CEA. The ability of such markers to predict the vulnerability of the plaque, as defined by the postoperative clinical observation [8], was then assessed via a receiver operating characteristic (ROC) curve analysis. The preliminary results have been presented at the Computing in Cardiology Conference 2024.

2. Materials and Methods

2.1. Experimental Protocol

One hundred patients with asymptomatic CAS of 70–99% scheduled for CEA were enrolled at the Department of Vascular Surgery of IRCCS Policlinico San Donato, San Donato Milanese, Milan, Italy. The study adhered to the Helsinki declaration for studies involving humans and was approved by the San Raffaele Hospital ethical committee (approval no. 110/int/2019, date 20 June 2019) and registered on ClinicalTrial.gov (Identifier: NCT05566080). Patients signed a written informed consent prior to participation.

Exclusion criteria were age under 18, non-sinus rhythm, presence of medical conditions for which survival expectancy was below 12 months, unstable or uncontrolled medical conditions (NYHA class III or IV heart failure or angina pectoris, previous cardiac surgery within 30 days, left ventricular ejection fraction below 30%, severe coronary artery disease with indication for surgery), medical history of stroke, or transient ischemic attack in the previous 6 months. After the exclusion of 22 patients for different reasons (bad signal recordings, missing data, previously unknown arrhythmias), 78 patients (age: 74.2 + 7.7 years, 27 females) were admitted to the analysis. Acquisition sessions were performed before surgery. After surgery, patients were divided in two classes: those with a vulnerable plaque (VULN) and those with a non-vulnerable plaque (STABLE) according to the presence of at least one of the following characteristics: ulceration, ruptured, or thin (<65 μm) fibrous cap, necrotic or lipidic core for more than 25% of the total area, large intraplaque hemorrhage, infiltration of inflammatory cells, neovascularization of the cap [8]. Hence, 36 patients were assigned to the VULN group and 42 to the STABLE one. The clinical features of the two groups are depicted in Table 1.

Table 1. Demographic and clinical parameters in STABLE and VULN patients.

Parameter	STABLE (*n* = 42)	VULN (*n* = 36)
age [yrs]	74.93 ± 7.30	73.39 ± 8.31
gender [female]	19 (45)	10 (28)
BMI [kg·m^{-2}]	25.96 ± 3.85	25.73 ± 4.20
hypertension	39 (93)	30 (83)

Table 1. *Cont.*

Parameter	STABLE (*n* = 42)	VULN (*n* = 36)
beta-blockers	13 (31)	13 (36)
diabetes	14 (33)	12 (33)
smoke	10 (24)	7 (19)
previous smoke	19 (45)	18 (50)
dyslipidemia	39 (93)	30 (83)
CAD	8 (19)	9 (25)
COPD	2 (5)	0 (0)
previous cerebrovascular events	3 (7)	6 (8)
% of stenosis	80.00 ± 4.42	80.28 ± 4.77

BMI = body mass index; CAD = coronary artery disease; COPD= chronic obstructive pulmonary disease. Continuous data are presented as mean ± standard deviation and categorical data as number (percentage).

2.2. Elastographic Markers Assessment

As described in [17], acquisition of pSWE was performed via an Esaote MyLab ultrasound system (EsaoteTM, Genova, Italy), with patients lying in supine position and with a slight neck extension in the region of the carotid artery. A probe working at 7.5 MHz and the Q-Elaxto software package (EsaoteTM, Genova, Italy) were used, while the quality arterial stiffness (QAS) software was used to derive arterial stiffness-related parameters through RF echo-based wall tracking. To perform acquisitions, the probe was placed along a longitudinal axis passing along the distal part of the carotid artery just below the atherosclerotic plaque. The QAS algorithm allowed us to automatically derive real-time measurements of the diameter change in the vessel between systolic and diastolic phases. The carotid pressure waveform was derived from the brachial pressure and cross-sectional area of the vessels during the cardiac cycle. From the ultrasound images, QAS allowed us to derive different markers of arterial stiffness from the changes in vessel area in relation to the local pressure during diastolic and systolic phases: (i) distensibility coefficient (DC), expressed in $1 \cdot kPa^{-1}$ and defined as $DC = \Delta A/(A \cdot \Delta p)$, where ΔA is the change in area during systole, A is the diastolic area of the vessel, and Δp is the local pulse pressure; (ii) compliance coefficient (CC), expressed in $mm^2 \cdot kPa^{-1}$ and defined as $DC = \Delta A/\Delta p$; (iii) index of alpha stiffness (α index), representing the elastic coefficient of the vessel calculated as $\alpha = A \cdot \ln(SAP/DAP)/\Delta A$, where SAP and DAP are, respectively, systolic and diastolic pressure, and ln is the natural logarithm; (iv) index of beta stiffness (β index), that is the elastic coefficient normalized by the vessel diameter, calculated as $\beta = D \cdot \ln(SAP/DAP)/\Delta D$, where D is the diastolic diameter and ΔD is the change in diameter during systole; (v) pulse wave velocity (PWV), calculated in $m \cdot s^{-1}$ as $PWV = 1/\sqrt{(\rho \cdot A - \Delta p/\Delta A)}$, where ρ is the blood density and Δp is the local pulse pressure; (vi) augmentation index (AIx), assessed as $AIx = [LocSAP - P(T1)/(LocSAP - LocDAP)] \times 100$, where LocSAP and LocDAP are local SAP and DAP and P(T1) is the pressure at the inflection points. Finally, the pSWE allowed us to compute the Young's elastic modulus (YM) of the plaque, expressed in kPa, representing the arterial stiffness [17,30].

2.3. Variability Series Extraction

Electrocardiogram (ECG) lead II (BioAmp, Adinstruments, Sydney, Australia) and noninvasive arterial pressure (AP) as derived from volume-clamp photopletysmography (CNAP, CNSystems, Graz, Austria) were recorded for 10 min with patients lying in supine position at REST and for 10 min during active standing (STAND). Signals were recorded at a sampling frequency of 400 Hz and synchronized with a polygraph (PowerLab, Adinstruments, Sydney, Australia). From the signals, we extracted the beat-to-beat time series of HP, taken as the time distance between two consecutive R-wave peaks of the ECG detected

with minimum jitters via parabolic interpolation, and of SAP, taken as the maximum of the AP signal within the HP. Respiration (RESP) was derived from the ECG amplitude modulations. Series of 256 consecutive beats for HP, SAP, and RESP were extracted during both REST and STAND and checked by a trained operator. Ectopic beats and misdetections were corrected by means of linear interpolation between the closest reliable values.

Mean values were extracted from the series, labeled as μ_{HP}, μ_{SAP}, and expressed in ms and mmHg. Then, after linear detrending of the series, variance of the time series was computed and, respectively, labeled as σ^2_{HP} and σ^2_{SAP} and expressed in ms^2 and $mmHg^2$.

Figure 1 shows the experimental setup.
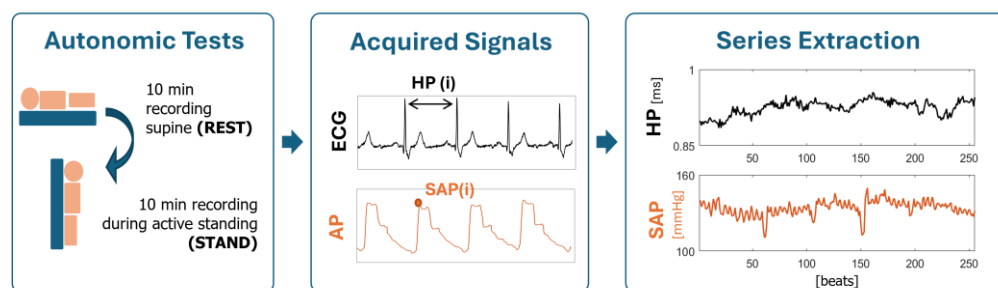
Figure 1. Experimental setup of cardiovascular signals acquisition. ECG = electrocardiogram; AP = arterial pressure; HP = heart period; SAP = systolic arterial pressure; i= ith beat; REST = at rest in supine position; STAND = during active standing.

2.4. Cardiovascular Control Markers Extraction

Consequently, the power spectral density of the series was computed to obtain univariate cardiovascular control spectral markers. The description of the dynamics was performed via an autoregressive model whose coefficients were identified via least squares method solved via Levinson–Durbin recursion. The number of coefficients was optimized via Akaike information criterion in the range 10–14 [31,32]. The power spectral density was factorized in spectral components. The area under each spectral component was computed via the residue theorem and the sum of the areas was equal to the variance of the series. Each component was labeled as low (LF, 0.04–0.15 Hz) or high (HF, 0.15–0.4 Hz) frequency according to the value of its central frequency [33]. The power of HP in the HF band in absolute units (HF_{HP}, expressed in ms^2) was associated to the vagal modulation directed to the ventricles [34], while the power of SAP in the LF band in absolute units (LFS_{AP}, expressed in $mmHg^2$) was depicted as a marker of sympathetic modulation directed to the vessels [19]. The respiratory frequency f_{RESP} was computed from the RESP series as the frequency at which the maximum in the HF band occurred.

Bivariate cross-spectral AR analysis was then used to derive baroreflex markers. Cross-spectral density function was computed from the parameters of the autoregressive bivariate model identified by solving the least squares problem via Cholesky decomposition, with the model order fixed to 10 [35]. The same method provided an estimation of the power spectral densities. The transfer function gain (TFG) was estimated as the ratio of the modulus of the cross-spectral density function from SAP to HP divided by the power spectral density of the input (e.g., SAP), while the squared coherence (K^2) was computed as the ratio of the square modulus of the cross-spectral density function to the product of the power spectral densities of SAP and HP. K^2 ranged between 0 and 1, where 0 means null and 1 full coupling. The TFG was sampled at the maximum of K^2 function in the LF and HF bands, and this value, expressed in $ms \cdot mmHg^{-1}$, was taken as a marker of baroreflex sensitivity, labeled, respectively, as BRS_{LF} and BRS_{HF} [36]. The K^2 was also sampled at its maximum in the LF and HF bands, and these markers, indicated as K^2_{LF} and K^2_{HF}, were taken as representative of the coupling between HP and SAP. The phase of

the cross-spectral density from SAP to HP in the LF and HF bands, expressed in rad and labeled as Ph_{LF} and Ph_{HF}, was used as representative of the phase shift from SAP to HP, where negative values indicate that HP lags behind SAP.

2.5. Statistical Analysis

Clinical and demographic data were compared between VULN and STABLE patients via t test, or Mann–Whitney rank sum test when appropriate in the case of continuous variables, and chi-square test, in the case of categorical variables. We utilized the t test or Mann–Whitney rank sum test when appropriate to compare the elastographic markers between the two groups. Two-way repeated measures analysis of variance (ANOVA) with one factor repetition was used to compute differences between the patient populations (VULN and STABLE) and experimental conditions (REST and STAND) of cardiovascular variability markers. Holm–Sidak test was used to assess multiple comparisons. Pearson's correlation coefficient was used to compute the relationship between elastographic and cardiovascular variability markers in STABLE and VULN patients. Analysis was carried out separately at REST and during STAND. The markers reporting a statistical difference between VULN and STABLE with $p < 0.01$ entered a multivariate logistic regression model. The regression coefficient, odds ratio, 95% confidence interval (CI), and type I error probability p of the multivariate regression model were computed. The area under the ROC curve (AUC) was assessed. The Youden index criterion was used to determine the best combination in terms of specificity and sensitivity and to assess the negative and positive predictive value (NPV and PPV).

3. Results

Table 1 depicts the clinical and demographic variables in STABLE and VULN patients. Remarkably, no differences were observed between the two populations.

Table 2 reports the results of elastographic markers assessed in the STABLE and VULN patients. Remarkably, only the YM of the plaque was significantly different between groups, being higher in STABLE plaque patients.

Table 2. Elastographic markers from QAS and pSWE in STABLE and VULN patients.

Index	STABLE	VULN
DC [$1 \cdot kPa^{-1}$]	0.010 ± 0.007	0.010 ± 0.006
CC [$mm^2 \cdot kPa^{-1}$]	0.595 ± 0.36	0.611 ± 0.335
α stiffness	11.239 ± 11.201	9.581 ± 5.188
β stiffness	22.742 ± 22.438	19.426 ± 10.4
PWV [$m \cdot s^{-1}$]	11.385 ± 5.105	11.058 ± 3.139
AIx [%]	8.195 ± 8.639	6.241 ± 5.412
YM [kPa]	46.211 ± 45.384	25.653 ± 27.237 *

DC = distensibility coefficient; CC = compliance coefficient; α stiffness = elastic coefficient of the vessel; β stiffness = elastic coefficient normalized on the diameter; PWV = pulse wave velocity; AIx = augmentation index; YM = Young's modulus of the plaque. STABLE = patients with a stable plaque; VULN = patients with a vulnerable plaque. The symbol * means $p < 0.05$ versus STABLE.

Table 3 shows markers of autonomic and cardiovascular control in the STABLE and VULN patients, assessed at REST and during STAND. μ_{HP} decreased at STAND as an effect of the postural challenge only in VULN patients. BRS_{HF} decreased during STAND in VULN patients with respect to REST and, at REST, resulted higher in VULN than in the STABLE patients. Remarkably, all the other indexes were not different between either group or condition.

Table 3. Autonomic and cardiovascular control markers in STABLE and VULN patients during REST and STAND.

Index	STABLE		VULN	
	REST	STAND	REST	STAND
μ_{HP} [ms]	882.92 ± 137.41	824.36 ± 185.92	924.75 ± 170.57	846.32 ± 227.07 *
σ^2_{HP} [ms^2]	581.86 ± 568.46	509.99 ± 506.19	687.05 ± 617.74	660.14 ± 639.33
HF_{HP} [ms^2]	153.98 ± 264.35	110.8 ± 161.11	157.97 ± 191.69	128.14 ± 179.63
LF_{HP}/HF_{HP}	1.36 ± 1.86	1.46 ± 1.64	6.77 ± 34.74	1.59 ± 1.84
f_{RESP} [Hz]	0.27 ± 0.04	0.27 ± 0.06	0.27 ± 0.04	0.28 ± 0.06
μ_{SAP} [mmHg]	147.44 ± 18.79	150.66 ± 29.94	144.35 ± 17.93	144.19 ± 31.34
σ^2_{SAP} [mmHg^2]	35.29 ± 30.43	35.49 ± 25.94	31.38 ± 32.82	36.04 ± 27.03
LF_{SAP} [mmHg^2]	4.35 ± 4.3	5.56 ± 7.53	4.06 ± 4.23	7.32 ± 10.41
α_{LF} [ms·mmHg^{-1}]	5.34 ± 4.64	5.46 ± 6.32	7.67 ± 9.35	5.29 ± 5.56
α_{HF} [ms·mmHg^{-1}]	4.97 ± 4.29	4.53 ± 3.74	6.91 ± 6.16	5.33 ± 5.38
K^2_{LF}	0.34 ± 0.18	0.33 ± 0.17	0.31 ± 0.19	0.36 ± 0.17
Ph_{LF} [rad]	-1.15 ± 1.37	-1.4 ± 1.21	-1.42 ± 1.22	-1.1 ± 1.28
BRS_{LF} [ms·mmHg^{-1}]	2.69 ± 1.98	2.35 ± 1.71	3.34 ± 2.85	2.64 ± 1.96
K^2_{HF}	0.63 ± 0.22	0.62 ± 0.27	0.62 ± 0.26	0.55 ± 0.26
Ph_{HF} [rad]	-0.32 ± 0.87	-0.25 ± 1.12	-0.26 ± 1.01	0.02 ± 0.98
BRS_{HF} [ms·mmHg^{-1}]	4.01 ± 4.12	3.42 ± 3.15	6.16 ± 6.19 §	3.81 ± 3.66 *

REST = at rest in supine position; STAND = during active standing; VULN = patients with vulnerable carotid plaque; STABLE = patients with stable carotid plaque; HP = heart period; SAP = systolic arterial pressure; μ = mean; σ^2 = variance; LF = low frequency; HF = high frequency. The symbol * indicates $p < 0.05$ with respect to REST. The symbol § indicates $p < 0.05$ with respect to STABLE.

Table 4 shows the results of the correlation between elastographic and autonomic and cardiovascular control markers assessed in STABLE patients. The majority of the autonomic and cardiovascular markers were not correlated with the elastographic markers, with the sole exception of the significant positive correlation of α_{LF} with AIx at REST.

Table 5 has the same structure as Table 4 but it refers to VULN patients. In this case, the number of significant correlations was larger. μ_{HP}, LF_{SAP} at REST, and μ_{HP}, μ_{SAP}, and σ^2_{SAP} during STAND were positively correlated with the plaque's YM. σ^2_{SAP} during REST was negatively correlated with DC and positively correlated with the PWV. The HF_{HP} during STAND was positively correlated with the markers related to the artery stiffness: α index, β index, and PWV. Finally, all the elastographic, autonomic, and cardiovascular control markers in Tables 2 and 3, taken separately at REST and during STAND, were compared between STABLE and VULN patients. The markers reporting a significance of the difference at the univariate level lower than 0.1 were selected to be entered in the following analyses. The chosen markers were the YM of the plaque and BRS_{HF} at REST.

A logistic regression analysis was performed to test the ability of plaque's YM and BRS_{HF} to predict the vulnerability of the plaque. The results of such analysis are presented in Table 6 in terms of odds ratio, 95% confidence interval (CI), p-value, and AUC. YM was significantly associated with the vulnerability of the plaque, reporting a p-value of 0.043 and an AUC of 0.625, while BRS_{HF} was less associated, reporting a p-value of 0.153 and an AUC of 0.616. The indexes then entered a multivariate logistic regression model, which reported an AUC equal to 0.694. The model was evaluated via the Youden Index criterion, reporting a sensitivity of 0.583 and a specificity of 0.833. The PPV was 80.3% and the NPV 63.2%. The ROC curve of the multivariate logistic model is shown in Figure 2.
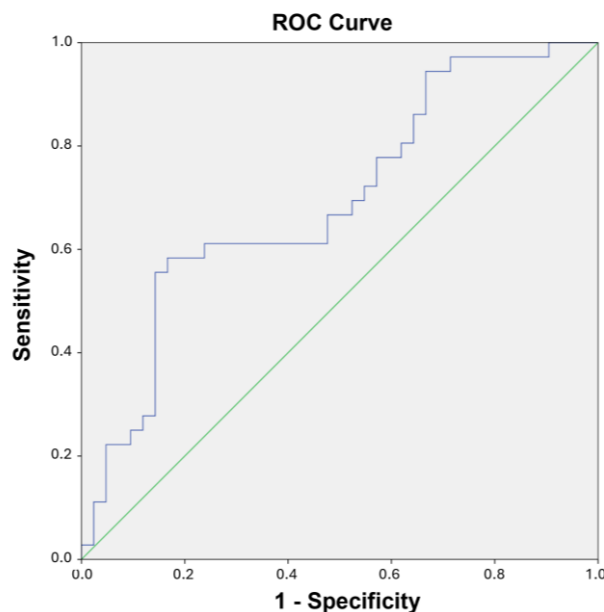
Figure 2. ROC curve related to the multivariate logistic regression model built with YM and BRS_{HF} evaluated at REST (blue). The green line represents the diagonal.

Table 4. Pearson's correlation coefficient r between elastographic and cardiovascular control markers in STABLE patients during REST and STAND.

Index	DC [1·kPa^{-1}]	CC [mm^2·kPa^{-1}]	α index	β index	PWV [m·s^{-1}]	AIx [%]	YM [kPa]
μ_{HP} REST [ms]	0.120	0.178	−0.217	−0.215	−0.257	−0.056	−0.007
σ^2_{HP} REST [ms^2]	−0.032	−0.040	−0.072	−0.072	−0.039	0.211	0.043
HF_{HP} REST [ms^2]	−0.030	−0.153	−0.108	−0.108	−0.026	0.153	−0.020
LF_{RR}/HF_{RR} REST	0.285	0.325	−0.160	−0.161	−0.209	−0.253	0.076
f_{RESP} REST [Hz]	0.0642	0.00808	0.2	0.0653	0.00353	0.00379	0.036
μ_{SAP} REST [mmHg]	−0.193	−0.256	0.066	0.068	0.172	0.148	−0.130
σ^2_{SAP} REST [mmHg^2]	0.143	0.193	−0.039	−0.041	−0.107	0.060	0.212
LF_{SAP} REST [mmHg^2]	−0.111	−0.035	0.170	0.169	0.138	−0.106	0.243
α_{LF} REST [ms·mmHg^{-1}]	−0.228	−0.211	0.084	0.084	0.173	0.349 *	0.076
α_{HF} REST [ms·mmHg^{-1}]	0.035	−0.099	−0.115	−0.114	−0.068	−0.052	0.017
K^2_{LF} REST	0.151	−0.022	−0.085	−0.085	−0.111	−0.235	−0.089
Ph_{LF} REST [rad]	−0.245	−0.031	0.128	0.129	0.133	0.256	0.237
BRS_{LF} REST [ms·mmHg^{-1}]	−0.198	−0.221	0.078	0.079	0.139	0.264	0.142
K^2_{HF} REST	0.302	0.095	−0.152	−0.152	−0.170	−0.274	−0.239
Ph_{HF} REST [rad]	0.276	0.171	−0.242	−0.240	−0.268	−0.248	−0.210
BRS_{HF} REST [ms·mmHg^{-1}]	0.139	0.097	−0.185	−0.184	−0.135	−0.140	−0.158
μ_{HP} STAND [ms]	0.011	0.093	−0.097	−0.094	−0.124	−0.003	0.056
σ^2_{HP} STAND [ms^2]	0.020	0.035	−0.083	−0.083	−0.082	−0.166	−0.028
HF_{HP} STAND [ms^2]	0.027	−0.158	−0.092	−0.092	−0.064	−0.166	−0.054
LF_{HP}/HF_{HP} STAND	−0.065	0.024	0.011	0.011	−0.009	0.207	−0.018
f_{RESP} STAND [Hz]	−0.0642	−0.0317	0.0125	−0.102	−0.118	−0.119	−0.0567
μ_{SAP} STAND [mmHg]	−0.246	−0.270	0.122	0.124	0.244	0.134	−0.061
σ^2_{SAP} STAND [mmHg^2]	0.091	0.309	−0.178	−0.178	−0.220	0.053	−0.155
LF_{SAP} STAND [mmHg^2]	0.014	0.086	−0.149	−0.149	−0.087	0.048	−0.088
α_{LF} STAND [ms·mmHg^{-1}]	−0.123	−0.269	0.146	0.145	0.127	−0.064	0.252
α_{HF} STAND [ms·mmHg^{-1}]	0.001	−0.121	−0.019	−0.020	−0.006	−0.196	0.103
K^2_{LF} STAND	0.124	0.063	0.049	0.048	−0.017	−0.033	−0.031
Ph_{LF} STAND [rad]	−0.204	−0.132	0.185	0.186	0.126	−0.091	0.235
BRS_{LF} STAND [ms·mmHg^{-1}]	−0.167	−0.214	0.228	0.228	0.187	−0.016	0.235
K^2_{HF} STAND	0.164	−0.081	−0.079	−0.080	−0.009	−0.046	0.011
Ph_{HF} STAND [rad]	0.123	0.051	−0.167	−0.164	−0.151	0.122	−0.093
BRS_{HF} STAND [ms·mmHg^{-1}]	−0.032	−0.069	0.028	0.027	0.057	−0.163	0.130

REST = at rest in supine position; STAND = during active standing; DC = distensibility coefficient; CC = compliance coefficient; α stiffness = stiffness, elastic coefficient of the vessel; β stiffness = elastic coefficient normalized on the diameter; PWV = pulse wave velocity; AIx = augmentation index; YM = Young's modulus of the plaque; HP = heart period; SAP = systolic arterial pressure; μ = mean; σ^2 = variance; LF = low frequency; HF = high frequency. The symbol * indicates significant correlation with $p < 0.05$.

Table 5. Pearson's correlation coefficient r between elastographic and cardiovascular control markers in VULN patients during REST and STAND.

Index	DC [1·kPa^{-1}]	CC [mm^2·kPa^{-1}]	α index	β index	PWV [m·s^{-1}]	AIx [%]	YM [kPa]
μ$_{HP}$ REST [ms]	−0.241	−0.133	0.108	0.108	0.179	−0.210	0.457 *
σ$^2_{HP}$ REST [ms^2]	−0.051	0.122	0.111	0.111	0.076	0.100	0.082
HF$_{HP}$ REST [ms^2]	−0.114	−0.005	0.176	0.176	0.121	0.003	0.178
LF$_{HP}$/HF$_{HP}$ REST	0.063	0.067	−0.127	−0.128	−0.089	−0.069	0.073
f$_{RESP}$ REST [Hz]	−0.282	0.044	−0.14	−0.18	0.174	0.173	0.24
μ$_{SAP}$ REST [mmHg]	−0.035	0.068	−0.077	−0.077	0.018	0.235	0.290
σ$^2_{SAP}$ REST [mmHg^2]	−0.309 *	−0.255	0.190	0.191	0.312 *	−0.048	0.190
LF$_{SAP}$ REST [mmHg^2]	−0.155	−0.150	0.090	0.091	0.180	−0.104	0.37 *
α$_{LF}$ REST [ms·mmHg^{-1}]	−0.021	0.093	−0.010	−0.010	−0.040	−0.075	−0.036
α$_{HF}$ REST [ms·mmHg^{-1}]	−0.006	0.047	−0.012	−0.012	−0.058	−0.090	−0.068
K$^2_{LF}$ REST	0.100	−0.001	−0.180	−0.180	−0.240	−0.092	−0.179
Ph$_{LF}$ REST [rad]	−0.143	−0.201	0.163	0.163	0.208	0.484 *	−0.011
BRS$_{LF}$ REST [ms·mmHg^{-1}]	0.105	0.109	−0.092	−0.093	−0.167	−0.076	−0.084
K$^2_{HF}$ REST	−0.110	−0.214	−0.008	−0.008	−0.035	0.171	−0.133
Ph$_{HF}$ REST [rad]	0.175	0.152	0.077	0.077	−0.062	−0.026	−0.287
BRS$_{HF}$ REST [ms·mmHg^{-1}]	−0.058	0.003	−0.046	−0.046	−0.056	−0.159	−0.095
μ$_{HP}$ STAND [ms]	−0.357 *	−0.258	0.152	0.153	0.274	−0.188	0.412 *
σ$^2_{HP}$ STAND [ms^2]	−0.175	−0.017	0.219	0.219	0.258	0.050	0.095
HF$_{HP}$ STAND [ms^2]	−0.289	−0.187	0.424 *	0.425 *	0.443 *	0.027	0.193
LF$_{HP}$/HF$_{HP}$ STAND	0.176	0.169	−0.199	−0.199	−0.198	−0.053	−0.061
f$_{RESP}$ STAND [Hz]	−0.0882	0.165	−0.201	−0.117	0.198	0.199	0.27
μ$_{SAP}$ STAND [mmHg]	−0.325 *	−0.345 *	0.096	0.097	0.117	−0.097	0.361 *
σ$^2_{SAP}$ STAND [mmHg^2]	−0.086	−0.071	−0.069	−0.069	−0.185	−0.157	0.328 *
LF$_{SAP}$ STAND [mmHg^2]	−0.068	−0.046	−0.057	−0.056	−0.033	−0.147	0.130
α$_{LF}$ STAND [ms·mmHg^{-1}]	−0.195	−0.122	0.119	0.120	0.149	0.185	−0.117
α$_{HF}$ STAND [ms·mmHg^{-1}]	−0.160	−0.032	0.300	0.300	0.295	0.167	−0.116
K$^2_{LF}$ STAND	0.119	0.031	−0.236	−0.236	−0.157	0.153	−0.065
Ph$_{LF}$ STAND [rad]	−0.167	−0.103	−0.005	−0.004	0.133	−0.156	0.037
BRS$_{LF}$ STAND [ms·mmHg^{-1}]	−0.035	0.127	−0.057	−0.057	−0.002	0.129	−0.159
K$^2_{HF}$ STAND	0.126	0.096	−0.192	−0.193	−0.174	0.232	0.154
Ph$_{HF}$ STAND [rad]	0.244	0.137	−0.121	−0.121	−0.264	0.083	0.013
BRS$_{HF}$ STAND [ms·mmHg^{-1}]	−0.109	0.048	0.088	0.088	0.108	0.001	−0.083

REST = at rest in supine position; STAND = during active standing; DC = distensibility coefficient; CC = compliance coefficient; α stiffness = stiffness, elastic coefficient of the vessel; β stiffness = elastic coefficient normalized on the diameter; PWV = pulse wave velocity; AIx = augmentation index; YM = Young's modulus of the plaque; HP = heart period; SAP = systolic arterial pressure; μ = mean; σ^2 = variance; LF = low frequency; HF = high frequency. The symbol * indicates significant correlation with $p < 0.05$.

Table 6. Results of multivariate logistic regression analysis for plaque's vulnerability prediction.

Parameter	Regression Coefficient	Odds Ratio	95% CI	*p*-Value	AUC
YM	−0.014	0.986	0.973–1.000	0.043	0.694
BRS$_{HF}$ REST	0.075	1.078	0.973–1.194	0.153	
constant	−0.038	0.963		0.928	

YM = Young's modulus of the plaque. BRS = baroreflex sensitivity; HF = high frequency; BRS$_{HF}$ = BRS in HF band evaluated at REST; CI = confidence interval; AUC = area under the ROC curve.

4. Discussion

The main findings of this work can be ~~resumed~~ summarized as follows: (i) in both STABLE and VULN groups, autonomic markers did not vary with orthostatic challenge, thus suggesting that the autonomic control is impaired; (ii) VULN patients had a lower YM; (iii) the VULN group's BRS$_{HF}$ decreased during STAND compared to REST, being higher at REST compared to the STABLE group; (iv) elastographic markers were significantly correlated with autonomic variability in VULN patients but not in the STABLE ones; (v) the joint analysis of Young's modulus and baroreflex markers improved the predictability of the plaque vulnerability.

4.1. Autonomic Control Is Impaired in Both Patients with Vulnerable and Stable Plaque

The assessment of autonomic function markers in patients with asymptomatic CAS allowed the detection of an autonomic impairment before the intervention, regardless of the kind of carotid plaque [25,26]. In fact, both STABLE and VULN populations did not present the expected response to the postural challenge in terms of a decrease of HF_{HP} and increase of LF_{SAP} [35–37]. The missing response to STAND confirmed the state of sympathetic activation and vagal withdrawal already suggested in patients featuring CAS [25,26]. Remarkably, plaque removal does not assure any improvement in the autonomic control likely because the surgical procedure could damage sensing areas of the carotid artery, with erroneous perception of the baroreflex loading [38,39].

4.2. Baroreflex Function at the Respiratory Rate Is Preserved in Patients with Vulnerable Plaque

One of the most interesting findings of this study is that at REST the BRS_{HF} was higher in the VULN group compared to the STABLE one, and it decreased, as expected [29,36], during STAND. This finding suggests that the baroreflex function could be more preserved in presence of a VULN plaque with respect to a STABLE one, since this population showed a better ability of modulating the baroreflex in response to the postural challenge compared to the STABLE group. Given this result, we suggest that subjects with STABLE plaque might be exposed to greater cardiovascular risk because they are less effective in compensating changes in SAP with suitable adaptations of HP, compared to VULN patients [18]. The greater stiffness of the substrate of the barosensitive areas where the mechanoreceptors are located might be responsible for the lower values of BRS_{HF} observed in the STABLE group compared to the VULN one. However, this speculation lacks appropriate direct evidence. Remarkably, at difference with the BRS_{HF}, the BRS_{LF} in the VULN group did not change with STAND. This finding might appear to be surprising given that BRS_{LF} is more reliable than BRS_{HF} in probing baroreflex function [36,40]. This greater statistical power of BRS_{HF} compared to BRS_{LF} in separating experimental conditions and groups might again support the concept that the observed impairment of baroreflex control in the STABLE group is more related to the mechanical transduction than the neural arch of cardiac baroreflex. Indeed, BRS_{HF} is more related to the ability of modifications of intrathoracic pressure during respiration [41] to solicit the site where the mechanoreceptors are located, being stiffer areas less able to sense modifications of arterial pressure.

4.3. The Relationship Between Elastographic and Autonomic Markers Is Different in Patients with Vulnerable or Stable Plaque

A preliminary study performed in a smaller population [17] allowed us to determine that patients with a vulnerable plaque could be differentiated from those with a stable one thanks to the assessment of elastographic markers and especially to the YM of the plaque, being lower in the VULN patients than in the STABLE ones. This work presents the same parameters in a larger population, confirming previous findings. In fact, YM was again the only marker able to differentiate populations, while the other markers related to arterial stiffness were not different between the two populations, being confirmed as a prognostic descriptor of the plaque's vulnerability. This ability of YM could be explained by the fact that the formation of the atherosclerotic plaque could lead to a change in the biomechanics of the vessel [42–44].

This study originally also presented a correlation analysis between elastographic and autonomic markers, performed separately in VULN and STABLE patients. In STABLE patients, we did not observe significant correlations, with the sole exception of an index of baroreflex function such as α_{LF} and index of arterial stiffness such as AIX. On the contrary, in VULN patients, we found several significant correlations between elastographic

and autonomic markers. In this group, the higher variability of markers of sympathetic modulation, such as σ^2_{SAP} and more specifically LF_{SAP}, might have favored the detection of a significant positive association with the YM of the plaque. This finding would suggest that patients with a more elastic plaque would be prone to having more variable and reactive cardiovascular control.

Furthermore, we found that in the VULN group, the higher the parasympathetic modulation directed to the heart during STAND, represented by HF_{HP}, the higher the stiffness of the carotid artery, represented by α, β index, and PWV. We suggest that within the group with the less remarkable value of stiffness, i.e., the VULN group, further differentiation can be carried out in terms of the response of the autonomic control to compensate greater stiffness values. In the STABLE group, any correlation is lost likely because the level of stiffness of the vasculature reached by this group prevents any correlation. Anyway, these findings can be considered only at a speculative level since, to our knowledge, a study exploring the association of elastographic and cardiovascular control markers has not been performed so far and should be confirmed in a control group, age and gender matched with our population.

4.4. The Joint Analysis of Autonomic and Elastographic Markers Improves the Predictability of Plaque Vulnerability

This work originally assessed the ability of both elastographic markers and cardiovascular control indexes to predict the vulnerability of the plaque via a logistic regression analysis. With respect to preliminary findings, this work assessed the ability of different elastographic markers to predict the vulnerability of the plaque. Anyway, only YM was found to be associated with plaque's vulnerability, with an AUC of 0.625 when used alone to predict the outcome. All the autonomic and cardiovascular control markers assessed at REST and STAND were tested for association with the plaque's vulnerability. Again, the marker able to discriminate VULN and STABLE with a probability of type-I error equal or lower to 0.1 was BRS_{HF} evaluated during REST, which was then tested first at the univariate level, entering a logistic regression analysis, reporting an AUC of 0.616. Remarkably, the multivariate logistic regression model built starting from the two markers reported a higher AUC, being equal to 0.694, further improving the results also in terms of positive and negative predictive value. These findings showed that the YM was the most powerful marker to discriminate plaque's vulnerability, but the addition of baroreflex analysis was shown to be able to increase the prediction ability.

Remarkably, since the performed analyses were noninvasive and preoperative, we suggest that they could be used in standard clinical practice to better determine the risk profile of the patients with asymptomatic CAS, thus helping clinicians in defining the better treatment for CAS patients by admitting to surgery only those with a higher risk of rupture of the plaque and, consequently, of stroke.

4.5. Limitations and Future Developments

We remark that this study did not consider comparisons with a proper control group, either made of healthy subjects or of symptomatic patients. It would be desirable in the future to provide reference values useful to scale the markers reported in this study. Furthermore, the presence of beta-blockers or other medications should also be considered in the model as confounding factors, given their ability to influence autonomic control. Novel therapies, in particular sodium-glucose co-transporter 2 (SGLT2) inhibitors, have been recently introduced, showing an efficacy to reduce vascular stiffness [45]. Future studies could be aimed at testing whether they have a synergistic effect with the markers proposed in this study. Furthermore, future studies will be depicted to enlarge the population and to test more advanced signal processing techniques to determine if the prediction can be

further improved. While confirmed, joint baroreflex and elastographic analysis to predict the vulnerability of the plaque could help in improving risk stratification in CAS patients and in tailoring therapies according to the risk of developing stroke.

5. Conclusions

This work originally presented a joint analysis of shear wave elastography, together with an RF-echo-based wall tracking method for arterial stiffness evaluation, autonomic function, and baroreflex control in CAS patients, to determine differences between those with STABLE and VULN carotid plaque. Remarkably, patients with VULN plaque, considered to be at higher clinical risk, presented a lower YM of the plaque and a preserved baroreflex response to the orthostatic challenge. Furthermore, as reported by a correlation analysis, a relation between elastographic and cardiovascular control markers was present only in this group. This work suggests that elastographic indexes are useful to predict the vulnerability of the plaque and that the addition of BRS indexes further improves the prediction, thus confirming the clinical value of baroreflex markers especially in asymptomatic CAS patients, as well as strengthening the validity of elastographic techniques.

Author Contributions: Conceptualization, V.B. and D.M.; methodology, V.B., G.M. and A.P.; software, V.B., A.P. and N.C.; validation, V.B., A.P. and D.M.; formal analysis, V.B., B.C., F.G. and N.C.; investigation, V.B., B.C., F.G., F.F. and D.M.; resources, D.M.; data curation, V.B., A.P. and D.M.; writing—original draft preparation, V.B., A.P. and D.M.; writing—review and editing, V.B., B.C., F.G., F.F., N.C., G.M., P.R., G.N., A.P. and D.M.; visualization, V.B. and A.P.; supervision, V.B., A.P. and D.M.; project administration, D.M.; funding acquisition, D.M. All authors have read and agreed to the published version of the manuscript.

Institutional Review Board Statement: The study adhered to the Helsinki declaration for studies involving humans and was approved by the San Raffaele Hospital ethical committee (approval no. 110/int/2019, date 20 June 2019) and registered on ClinicalTrial.gov (Identifier: NCT05566080).

Informed Consent Statement: Informed consent was obtained from all subjects involved in the study.

Data Availability Statement: Data are available upon reasonable request to the corresponding author.

Conflicts of Interest: The authors declare no conflicts of interest.

References

1. Chang, R.W.; Tucker, L.; Rothenberg, K.A.; Lancaster, E.; Faruqi, R.M.; Kuang, H.C.; Flint, A.C.; Avins, A.L.; Nguyen-Huynh, M.N. Incidence of Ischemic Stroke in Patients with Asymptomatic Severe Carotid Stenosis Without Surgical Intervention. *JAMA* **2022**, *327*, 1974–1982. [CrossRef] [PubMed]
2. Bonati, L.H.; Jansen, O.; de Borst, G.J.; Brown, M.M. Management of atherosclerotic extracranial carotid artery stenosis. *Lancet Neurol.* **2022**, *21*, 273–283. [CrossRef] [PubMed]
3. Spence, J.D. Endarterectomy vs. stenting vs. medical therapy. *Int. J. Stroke* **2016**, *11*, 500–501. [CrossRef] [PubMed]
4. Paraskevas, K.I.; Nicolaides, A.N.; Suri, J.S.; Saba, L. Identifying the Vulnerable Carotid Atherosclerotic Plaque in Patients with Asymptomatic Carotid Stenosis. *Angiology* **2022**, *73*, 93–95. [CrossRef] [PubMed]
5. Gupta, A.; Baradaran, H.; Schweitzer, A.D.; Kamel, H.; Pandya, A.; Delgado, D.; Dunning, A.; Mushlin, A.I.; Sanelli, P.C. Carotid plaque MRI and stroke risk: A systematic review and meta-analysis. *Stroke* **2013**, *44*, 3071–3077. [CrossRef] [PubMed]
6. Yao, Y.; Zhang, P. Novel ultrasound techniques in the identification of vulnerable plaques-an updated review of the literature. *Front. Cardiovasc. Med.* **2023**, *10*, 1069745. [CrossRef]
7. Mazzaccaro, D.; Dolci, M.; Perego, F.; Delbue, S.; Giannetta, M.; Cardani, R.; Renna, L.V.; Costa, E.; Corsi-Romanelli, M.M.; Galli, C.; et al. Viral Agents and Systemic Levels of Inflammatory Cytokines in Vulnerable and Stable Atherosclerotic Carotid Plaques. *Ann. Vasc. Surg.* **2022**, *82*, 325–333. [CrossRef]
8. Lovett, J.K.; Gallagher, P.J.; Hands, L.J.; Walton, J.; Rothwell, P.M. Histological correlates of carotid plaque surface morphology on lumen contrast imaging. *Circulation* **2004**, *110*, 2190–2197. [CrossRef]

9.   Kolos, I.; Troitskiy, A.; Balakhonova, T.; Shariya, M.; Skrypnik, D.; Tvorogova, T.; Deev, A.; Boytsov, S.; Akezheva, L.R.; Dupik, N.V.; et al. Modern medical treatment with or without carotid endarterectomy for severe asymptomatic carotid atherosclerosis. *J. Vasc. Surg.* **2015**, *62*, 914–922. [CrossRef]

10. Turi, V.; Dragan, S.; Iurciuc, M.; Moleriu, L.; Bungau, S.; Tit, D.M.; Toader, D.; Diaconu, C.C.; Behl, T.; Petre, I. Arterial Function in Healthy Pregnant Women vs. Non-Pregnant Women—A 10-Year Study. *Diagnostics* **2020**, *10*, 374. [CrossRef]

11. Saba, L.; Mossa-Basha, M.; Abbott, A.; Lanzino, G.; Wardlaw, J.M.; Hatsukami, T.S.; Micheletti, G.; Balestrieri, A.; Hedin, U.; Moody, A.R.; et al. Multinational Survey of Current Practice from Imaging to Treatment of Atherosclerotic Carotid Stenosis. *Cerebrovasc. Dis.* **2021**, *50*, 108–120. [CrossRef] [PubMed]

12. Davidhi, A.; Rafailidis, V.; Destanis, E.; Prassopoulos, P.; Foinitsis, S. Ultrasound Elastography: Another piece in the puzzle of carotid plaque vulnerability? *Med. Ultrason.* **2022**, *24*, 356–363. [CrossRef] [PubMed]

13. Mahmood, B.; Ewertsen, C.; Carlsen, J.; Nielsen, M.B. Ultrasound Vascular Elastography as a Tool for Assessing Atherosclerotic Plaques—A Systematic Literature Review. *Ultrasound Int. Open* **2016**, *2*, E106–E112. [CrossRef] [PubMed]

14. Helderman, F.; Segers, D.; de Crom, R.; Hierck, B.P.; Poelmann, R.E.; Evans, P.C.; Krams, R. Effect of shear stress on vascular inflammation and plaque development. *Curr. Opin. Lipidol.* **2007**, *18*, 527–533. [CrossRef]

15. Ramnarine, K.V.; Garrard, J.W.; Kanber, B.; Nduwayo, S.; Hartshorne, T.C.; Robinson, T.G. Shear wave elastography imaging of carotid plaques: Feasible, reproducible and of clinical potential. *Cardiovasc. Ultrasound* **2014**, *12*, 49. [CrossRef]

16. Goudot, G.; Sitruk, J.; Jimenez, A.; Julia, P.; Khider, L.; Alsac, J.; El Batti, S.; Bruneval, P.; Amemyia, K.; Pedreira, O.; et al. Carotid Plaque Vulnerability Assessed by Combined Shear Wave Elastography and Ultrafast Doppler Compared to Histology. *Transl. Stroke Res.* **2022**, *13*, 100–111. [CrossRef]

17. Mazzaccaro, D.; Giannetta, M.; Fancoli, F.; Matrone, G.; Curcio, N.; Conti, M.; Righini, P.; Nano, G. Role of Preoperative Ultrasound Shear-Wave Elastography and Radiofrequency-Based Arterial Wall Tracking in Assessing the Vulnerability of Carotid Plaques: Preliminary Results. *Diagnostics* **2023**, *13*, 805. [CrossRef]

18. La Rovere, M.T.; Bigger, J.J.T.; Marcus, F.I.; Mortara, A.; Schwartz, P.J. Baroreflex sensitivity and heart-rate variability in prediction of total cardiac mortality after myocardial infarction. ATRAMI (Autonomic Tone and Reflexes After Myocardial Infarction) Investigators. *Lancet* **1998**, *351*, 478–484. [CrossRef]

19. Bari, V.; Ranucci, M.; De Maria, B.; Cairo, B.; Pistuddi, V.; Porta, A. Model-based directional analysis of cardiovascular variability identifies patients developing atrial fibrillation after coronary artery bypass grafting. *Int. J. Cardiol.* **2018**, *258*, 97–102. [CrossRef]

20. Waldstein, S.R.; Siegel, E.L.; Lefkowitz, D.; Maier, K.J.; Brown, J.R.; Obuchowski, A.M.; Katzel, L.I. Stress-induced blood pressure reactivity and silent cerebrovascular disease. *Stroke* **2004**, *35*, 1294–1298. [CrossRef]

21. Goldstein, I.B.; Bartzokis, G.; Hance, D.B.; Shapiro, D. Relationship between blood pressure and subcortical lesions in healthy elderly people. *Stroke* **1998**, *29*, 765–772. [CrossRef] [PubMed]

22. Tsai, W.; Lin, H.; Lai, Y.; Hsu, C.; Huang, C.; Wang, H.; Su, C.; Su, Y.; Lin, W.; Cheng, B.; et al. The Effect of Stroke Subtypes on Baroreceptor Sensitivity, a Predict for Acute Stroke Outcome. *Biomed. Res. Int.* **2019**, *2019*, 7614828. [CrossRef] [PubMed]

23. Yperzeele, L.; van Hooff, R.; Nagels, G.; De Smedt, A.; De Keyser, J.; Brouns, R. Heart rate variability and baroreceptor sensitivity in acute stroke: A systematic review. *Int. J. Stroke* **2015**, *10*, 796–800. [CrossRef] [PubMed]

24. Colivicchi, F.; Bassi, A.; Santini, M.; Caltagirone, C. Prognostic implications of right-sided insular damage, cardiac autonomic derangement, and arrhythmias after acute ischemic stroke. *Stroke* **2005**, *36*, 1710–1715. [CrossRef]

25. Marrocco-Trischitta, M.; Cremona, G.; Lucini, D.; Natali-Sora, M.; Cursi, M.; Cianflone, D.; Pagani, M.; Chiesa, R. Peripheral baroreflex and chemoreflex function after eversion carotid endarterectomy. *J. Vasc. Surg.* **2013**, *58*, 136–144.e1. [CrossRef]

26. Vecchia, L.D.; Barbic, F.; Galli, A.; Pisacreta, M.; Gornati, R.; Porretta, T.; Porta, A.; Furlan, R. Favorable effects of carotid endarterectomy on baroreflex sensitivity and cardiovascular neural modulation: A 4-month follow-up. *Am. J. Physiol. Regul. Integr. Comp. Physiol.* **2013**, *304*, 1114. [CrossRef]

27. Kadoya, M.; Koyama, H.; Kurajoh, M.; Kanzaki, A.; Kakutani-Hatayama, M.; Okazaki, H.; Shoji, T.; Moriwaki, Y.; Yamamoto, T.; Emoto, M.; et al. Sleep, cardiac autonomic function, and carotid atherosclerosis in patients with cardiovascular risks: HSCAA study. *Atherosclerosis* **2015**, *238*, 409–414. [CrossRef]

28. Bertinieri, G.; Di Rienzo, M.; Cavallazzi, A.; Ferrari, A.U.; Pedotti, A.; Mancia, G. Evaluation of baroreceptor reflex by blood pressure monitoring in unanesthetized cats. *Am. J. Physiol.* **1988**, *254*, 377.

29. De Maria, B.; Bari, V.; Cairo, B.; Vaini, E.; Esler, M.; Lambert, E.; Baumert, M.; Cerutti, S.; Vecchia, L.D.; Porta, A. Characterization of the Asymmetry of the Cardiac and Sympathetic Arms of the Baroreflex From Spontaneous Variability During Incremental Head-Up Tilt. *Front. Physiol.* **2019**, *10*, 342. [CrossRef]

30. Meinders, J.M.; Hoeks, A.P.G. Simultaneous assessment of diameter and pressure waveforms in the carotid artery. *Ultrasound Med. Biol.* **2004**, *30*, 147–154. [CrossRef]

31. Kay, S.M. *Spectrum Analysis: A Modern Perspective*; Prentice Hall: Englewood Cliffs, NJ, USA, 1988.

32. Akaike, H. A new look at the statistical model identification. *IEEE Trans. Autom. Control* **1974**, *19*, 716–723. [CrossRef]

33. Baselli, G.; Cerutti, S.; Civardi, S.; Lombardi, F.; Malliani, A.; Merri, M.; Pagani, M.; Rizzo, G. Heart rate variability signal processing: A quantitative approach as an aid to diagnosis in cardiovascular pathologies. *Int. J. Biomed. Comput.* **1987**, *20*, 51–70. [CrossRef] [PubMed]

34. Akselrod, S.; Gordon, D.; Ubel, F.A.; Shannon, D.C.; Berger, A.C.; Cohen, R.J. Power spectrum analysis of heart rate fluctuation: A quantitative probe of beat-to-beat cardiovascular control. *Science* **1981**, *213*, 220–222. [CrossRef] [PubMed]

35. Milan-Mattos, J.C.; Porta, A.; Perseguini, N.M.; Minatel, V.; Rehder-Santos, P.; Takahashi, A.C.M.; Mattiello, S.M.; Catai, A.M. Influence of age and gender on the phase and strength of the relation between heart period and systolic blood pressure spontaneous fluctuations. *J. Appl. Physiol.* **2018**, *124*, 791–804. [CrossRef] [PubMed]

36. Bari, V.; Vaini, E.; Pistuddi, V.; Fantinato, A.; Cairo, B.; De Maria, B.; Vecchia, L.A.D.; Ranucci, M.; Porta, A. Comparison of Causal and Non-causal Strategies for the Assessment of Baroreflex Sensitivity in Predicting Acute Kidney Dysfunction After Coronary Artery Bypass Grafting. *Front. Physiol.* **2019**, *10*, 1319. [CrossRef]

37. Pomeranz, B.; Macaulay, R.J.; Caudill, M.A.; Kutz, I.; Adam, D.; Gordon, D.; Kilborn, K.M.; Barger, A.C.; Shannon, D.C.; Cohen, R.J. Assessment of autonomic function in humans by heart rate spectral analysis. *Am. J. Physiol.* **1985**, *248*, 151. [CrossRef]

38. Demirci, M.; Saribaş, O.; Uluç, K.; Cekirge, S.; Böke, E.; Ay, H. Carotid artery stenting and endarterectomy have different effects on heart rate variability. *J. Neurol. Sci.* **2006**, *241*, 45–51. [CrossRef]

39. Demirel, S.; Attigah, N.; Bruijnen, H.; Macek, L.; Hakimi, M.; Able, T.; Böckler, D. Changes in baroreceptor sensitivity after eversion carotid endarterectomy. *J. Vasc. Surg.* **2012**, *55*, 1322–1328. [CrossRef]

40. De Boer, R.W.; Karemaker, J.M.; Strackee, J. Relationships between short-term blood-pressure fluctuations and heart-rate variability in resting subjects. I: A spectral analysis approach. *Med. Biol. Eng. Comput.* **1985**, *23*, 352–358. [CrossRef]

41. Toska, K.; Eriksen, M. Respiration-synchronous fluctuations in stroke volume, heart rate and arterial pressure in humans. *J. Physiol.* **1993**, *472*, 501–512. [CrossRef]

42. Di Leo, N.; Venturini, L.; de Soccio, V.; Forte, V.; Lucchetti, P.; Cerone, G.; Alagna, G.; Caratozzolo, M.; Messineo, D.; Di Gioia, C.; et al. Multiparametric ultrasound evaluation with CEUS and shear wave elastography for carotid plaque risk stratification. *J. Ultrasound* **2018**, *21*, 293–300. [CrossRef] [PubMed]

43. Garrard, J.W.; Ummur, P.; Nduwayo, S.; Kanber, B.; Hartshorne, T.C.; West, K.P.; Moore, D.; Robinson, T.G.; Ramnarine, K.V. Shear Wave Elastography May Be Superior to Greyscale Median for the Identification of Carotid Plaque Vulnerability: A Comparison with Histology. *Ultraschall Med.* **2015**, *36*, 386–390. [CrossRef] [PubMed]

44. Dhawan, S.S.; Nanjundappa, R.P.A.; Branch, J.R.; Taylor, W.R.; Quyyumi, A.A.; Jo, H.; McDaniel, M.C.; Suo, J.; Giddens, D.; Samady, H. Shear stress and plaque development. *Expert. Rev. Cardiovasc. Ther.* **2010**, *8*, 545–556. [CrossRef] [PubMed]

45. Stachteas, P.; Karakasis, P.; Patoulias, D.; Clemenza, F.; Fragakis, N.; Rizzo, M. The effect of sodium-glucose co-transporter-2 inhibitors on markers of subclinical atherosclerosis. *Ann. Med.* **2023**, *55*, 2304667. [CrossRef] [PubMed]